INTERNATIONAL JOURNAL FOR NUMERICAL METHODS IN ENGINEERING, VOL. 30, 875–898 (1990)

FIXED GRID TECHNIQUES FOR PHASE CHANGE PROBLEMS: A REVIEW

V. R. VOLLER AND C. R. SWAMINATHAN

Mineral Resources Research Center, Department of Civil and Mineral Engineering, University of Minnesota, Minneapolis, MN 55455, U.S.A.

B. G. THOMAS

Department of Mechanical and Industrial Engineering, University of Illinois at Urbana-Champaign, Urbana, IL 61801, U.S.A.

SUMMARY

The aim of this paper is to categorize the major fixed grid formulations and solution methods for conduction controlled phase change problems. Using a two phase model of a solid/liquid phase change, the basic enthalpy equation is derived. Starting from this equation, a number of alternative formulations are obtained. All the formulations are reduced to a standard form. From this standard form, finite element and finite volume discretizations are developed. These discretizations are used as the basis for a number of fixed grid numerical solution techniques for solidification phase change systems. In particular, various apparent capacity and source based enthalpy methods are explored.

INTRODUCTION

Background

Many important physical processes, including both solid/liquid transformations and solid state transformations, involve phase change. The emphasis in the numerical modelling of such systems centres on the treatment of the latent heat evolution. The numerical treatment of this non-linear phenomenon poses many problems and many alternative solution methods have been proposed. An excellent survey of the various techniques can be found in Crank.[1]

A popular approach for the numerical modelling of phase change systems is the so called 'fixed' grid methods.[1–8] The essential feature of these methods is that the latent heat evolution is accounted for in the governing energy equation by defining either a total enthalpy, H, an effective specific heat coefficient, c^{A}, or a heat source term, Q. Consequently, the numerical solution can be carried out on a space grid that remains fixed throughout the calculation.

The major advantage of fixed grid methods is that the numerical treatment of the phase change can be achieved through simple modifications of existing heat transfer numerical methods and/or software. As such, fixed grid methods have been successful in modelling a variety of complex phase change systems involving arbitrary three-dimensional domains and multiple phenomena, e.g. convective transport,[6–9] solute transport,[10–12] stress evolution,[13] microstructure evolution.[8,14,15]

0029–5981/90/120875–24$12.00

Received January 1990

Scope of the present work

The object of this paper is to provide a comprehensive review of available fixed grid methods for the numerical modelling and analysis of phase change systems. Emphasis will be directed at the numerical features that result from the solution of phase change systems as opposed to an analysis of the underlying physics. In this investigation, the aim *is not* to identify a single best method or class of methods. The authors recognize that the choice of method will depend on the context of the problem and the personal preference of the investigator. In essence, the current paper will provide a full range of fixed grid techniques from which a given investigator can choose an approach appropriate to the problem at hand.

For clarity of presentation, this work will focus on solidification phase change systems controlled by transient heat conduction. This choice is justified on noting that the major numerical difficulties and features of fixed grid phase change techniques are manifest in such systems.

THE GOVERNING EQUATION

The nature of a solidification phase change can take many forms. An attempt to classify the possibilities is presented in Figure 1. This classification is based on the state of a small portion of the material in the phase change region, representing a single degree of freedom in the numerical discretization. Three classes of phase change are identified:

Case (a). Distinct: The phase change region consists of distinct solid and liquid phases separated by a smooth continuous front; for example the freezing of water or rapid solidification of pure metals.

Case (b). Alloy: The phase change region has a crystalline structure consisting of columnar and/or equi-axed grains and the solid/liquid interface is a complex shape not necessarily smooth or continuous; for example the solidification of most metal alloys.

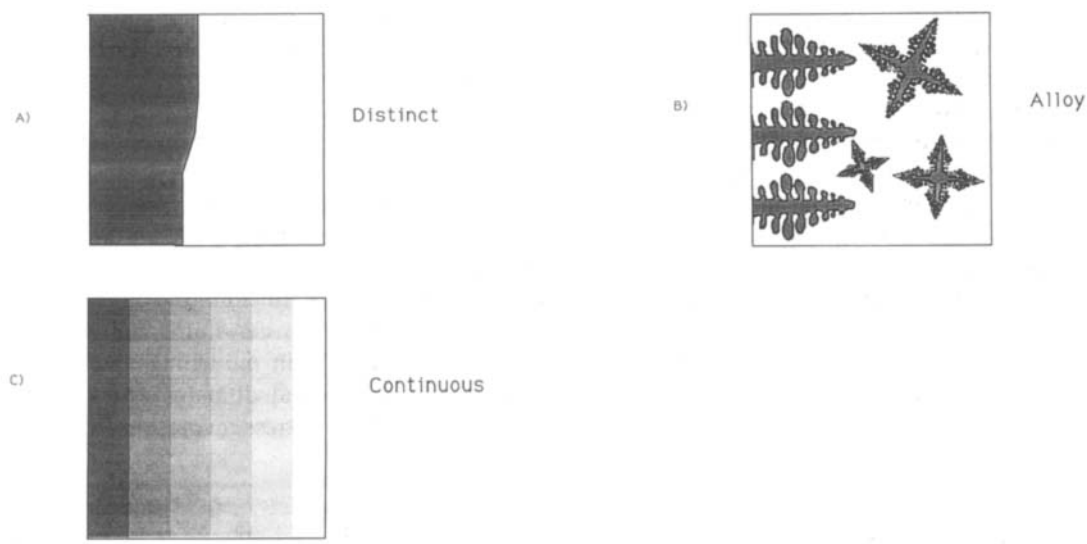

Figure 1. Classification of solidification phase change

Case (c). Continuous: The liquid and solid phases are fully dispersed throughout the phase change region and at the chosen scale there is no distinct interface between the solid and liquid phases; for example the solidification of wax, polymers or glasses.

In a distinct phase change, case (a), the state of the system is conveniently characterized by the position of the interface. In such cases the class of so called 'front tracking' methods[1] offer an alternative solution approach to fixed grid methods. However, as the solid/liquid interface becomes less distinct (cases (b) and (c)), front tracking becomes computationally expensive if not impossible. In such cases, we feel that characterization of the phase change is best achieved by a model based on the phase fractions. Further, models of this nature are more easily numerically implemented using a fixed grid method.

In the development of a governing equation for solidification phase change systems suitable for implementation on a fixed grid, we select the alloy phase change, case (b), as a representative system. (Note that with this choice the distinct and continuous phase changes can be viewed as special cases.) As demonstrated by Beckermann,[16] the appropriate governing equation can be rigorously derived using a local volume averaged model of the two phase solid and liquid region.[16-18] This model is based on performing microscopic balances on the transport of enthalpy in the distinct solid and liquid fractions contained in a small 'representative elementary volume' (REV). On integrating the resulting solid and liquid microscopic equations over the chosen REV, applying a number of integral identities[17,18] and assuming a constant REV temperature $T = T_s = T_l$ and small local velocity fluctuations, averaged equations are obtained,

$$\frac{\partial}{\partial t}(g_s H_s) + \nabla\cdot(g_s H_s \mathbf{u}_s) - \nabla\cdot(g_s k_s \nabla T) + (\text{interface term})_s = 0 \tag{1a}$$

$$\frac{\partial}{\partial t}(g_l H_l) + \nabla\cdot(g_l H_l \mathbf{u}_l) - \nabla\cdot(g_l k_l \nabla T) + (\text{interface term})_l = 0 \tag{1b}$$

where the subscript $[\,]_s$ and $[\,]_l$ refer to the solid and liquid phases respectively. With the appropriate subscript, g is the phase volume fraction, k is the phase conductivity, $\mathbf{u}$ is the phase velocity and H is the phase enthalpy. In equation (1), the enthalpies and velocities are intrinsic phase averages e.g.

$$H_s(\mathbf{X}, t) = \frac{1}{V_s}\int H_s^*(\mathbf{x}, t)\,\mathrm{d}V_s \tag{2}$$

where V_s is the volume of the solid fraction in the REV, $\mathbf{x}$ is the position vector of points in the solid, $H_s^*(\mathbf{x}, t)$ is the value of the solid enthalpy at this point and $\mathbf{X}$ is the position vector of the centroid of the REV. In the current case, since the REV is isothermal, specific heats, c_s and c_l, can be defined such that

$$H_s = \int_{T_{ref}}^{T} \rho_s c_s\,\mathrm{d}\theta \tag{3a}$$

$$H_l = \int_{T_{ref}}^{T} \rho_l c_l\,\mathrm{d}\theta + \rho_l L \tag{3b}$$

where ρ is the density and L is the latent heat of solidification.

On assuming that only two phases are present (i.e. phenomena such as porosity formation are neglected), so that $g_l = 1 - g_s$, it is convenient to additively combine equations (1). In this step, the interface terms cancel out (essentially they represent a generalized Stefan condition) and a

single governing enthalpy equation results,

$$\frac{\partial}{\partial t}(H) + \nabla\cdot(g_s H_s \mathbf{u}_s + g_l H_l \mathbf{u}_l) = \nabla\cdot(k\nabla T) \tag{4}$$

On neglecting convection effects (e.g. due to density change at the phase interface or density variations in the liquid phase) equation (4) becomes

$$\frac{\partial}{\partial t}(H) = \nabla\cdot(k\nabla T) \tag{5}$$

where k is a 'mixture' conductivity given as

$$k = g_s k_s + g_l k_l \tag{6}$$

and H is a 'mixture' enthalpy given as[12]

$$H = g_s \int_{T_{ref}}^{T} \rho_s c_s \, d\theta + g_l \int_{T_{ref}}^{T} \rho_l c_l \, d\theta + \rho_l g_l L \tag{7}$$

where T_{ref} is an arbitrary reference temperature.

In the absence of heat generation due to compressibility or viscous dissipation, equation (5) is suitable for the description of a general conduction controlled phase change system. Note that it is similar in form to the enthalpy equation given in Crank.[1] Recognize, however, that the definition of the mixture enthalpy, H, will mean that the equation is valid across the range of phase change systems illustrated in Figure 1.

A key feature in the development of fixed grid methods, based on equation (5), is the definition of the local liquid volume fraction, g_l. In general the local liquid fraction will depend on the nature of solidification. If the kinetics of the transformation are such that under-cooling is significant, g_l could be a function of temperature, cooling rate, solidification speed and nucleation rate.[8,14,15] In a multi-component alloy, solutal transport (macro-segregation) will also influence the local liquid fraction field.[10–12] To simplify and focus subsequent discussions in the current work, the liquid fraction is taken to be a function of temperature alone, i.e.

$$g_l = F(T) \tag{8}$$

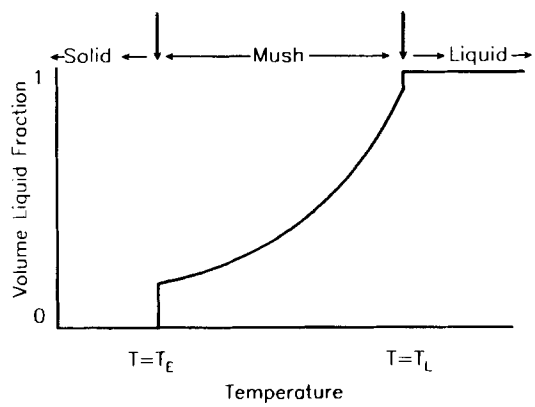

Figure 2. A general liquid fraction–temperature curve

This is justified on noting that in many systems kinetic under-cooling is small and macro-segregation is principally driven by convection transport. A general form of the liquid fraction versus temperature function, $F(T)$, is shown in Figure 2. Referring to the two phase solid and liquid zone as the 'mushy' region, important features in this plot are

(i) a temperature range associated with a non-linear change of g_l in the mushy region;
(ii) a step discontinuity at the 'mush/solid' interface that can be associated with an eutectic phase change; and
(iii) a step discontinuity at the 'liquid/mush' interface which can be used to approximately represent a kinetic under-cooling at the dendrite tips.[19]

ALTERNATIVE FORMS OF THE GOVERNING EQUATION

The given governing equation (5) is non-linear in that it contains two related but unknown variables, H and T. In seeking a numerical solution it is often convenient, although not necessary, to reformulate the governing equation in terms of a single unknown variable with the non-linear latent heat effects 'isolated' in a source term or a coefficient.

Apparent heat capacity

On taking the derivative of H with respect to temperature, T, we can define an apparent specific heat as

$$c^{\mathrm{A}} = \frac{\mathrm{d}H}{\mathrm{d}T} \tag{9a}$$

or, using equation (7),

$$c^{\mathrm{A}} = c_{\mathrm{vol}} + \delta H \frac{\mathrm{d}g_l}{\mathrm{d}T} \tag{9b}$$

where

$$c_{\mathrm{vol}} = g_s \rho_s c_s + g_l \rho_l c_l \tag{10}$$

and

$$\delta H = \int_{T_{\mathrm{ref}}}^{T} (\rho_l c_l - \rho_s c_s)\mathrm{d}\theta + \rho_l L \tag{11}$$

is the difference between the liquid and solid enthalpies (i.e. $H_l - H_s$). On noting that

$$\frac{\partial H}{\partial t} = \frac{\mathrm{d}H}{\mathrm{d}T}\frac{\partial T}{\partial t} \tag{12}$$

appropriate substitution into equation (5) results in

$$c^{\mathrm{A}} \frac{\partial T}{\partial t} = \nabla \cdot (k \nabla T) \tag{13}$$

This equation is often referred to as the enhanced or apparent heat capacity equation. It is identical in form to the basic Fourier heat conduction equation. As a result, the formulation can be easily incorporated into existing codes. With reference to such a numerical implementation two points are made concerning the evaluation of the apparent heat capacity, c^{A}.

1. As noted in Figure 2, the liquid fraction curve $g_l(T)$ may contain 'jump' discontinuities. In a strict mathematical context, equation (9) cannot be used to evaluate c^A at such discontinuities. In practice this problem is overcome on introducing small artificial temperature ranges at the jumps, thus ensuring that $g_l(T)$ is at least piecewise continuous throughout the temperature domain.
2. The apparent heat capacity, c^A, given in equation (9), is highly dependent on both space and time. In practice, this requires that care be taken to develop an effective means of numerically approximating equation (9).[20–26]

More details on the numerical implementation of apparent heat capacity methods will be furnished in the discussion of the numerical solution approaches.

The latent heat source term

An alternative to introducing a non-linear coefficient in the form of a specific heat is to develop a non-linear source term in the governing equation. In the finite difference (control volume) literature such approaches are referred to as 'source term' techniques.[6,9,27] In the finite element literature they are referred to as 'fictitious heat flow' or 'budget node' methods.[28,29] In essence, on using equation (7), the term $\partial H/\partial t$ can be expanded as

$$\frac{\partial H}{\partial t} = c_{vol}\frac{\partial T}{\partial t} + \delta H\frac{\partial g_l}{\partial t} \tag{14}$$

where for simplicity and convenience temporal changes in the liquid density have been ignoted. Substitution of equation (14) in equation (5) results in

$$c_{vol}\frac{\partial T}{\partial t} = \nabla\cdot(k\nabla T) + S \tag{15}$$

where

$$S = -\delta H\frac{\partial g_l}{\partial t} \tag{16}$$

Equation (15) is also in a form which is compatible with basic numerical solution approaches, in particular those based on finite difference control volumes.[30] Further, unlike the apparent heat capacity formulation, equation (15) can deal with the general liquid fraction curve depicted in Figure 2 without the need for artificial temperature ranges.

In essence, equation (15) is not constructed in terms of a single variable since the liquid fraction field, g_l, appearing in the source term is an unknown along with the temperature field. In a numerical solution this problem is overcome on appropriate iteration. The key feature in such a numerical solution is the way in which the liquid fraction field is updated on each iteration.[6,9,27] Techniques for updating g_l will be discussed in the numerical solution section.

The Kirchhoff transformation

In using the above formulations, difficulties may arise in the numerical discretizations when the conductivity is dependent on temperature. A means around this is to reformulate the problem in terms of the Kirchhoff temperature defined as[1]

$$\psi = \int_{T_{ref}}^{T} k(\theta)\,\mathrm{d}\theta \tag{17}$$

Note that with this definition

$$\nabla\psi = k\nabla T$$

and

$$\frac{\partial\psi}{\partial t} = k\frac{\partial T}{\partial t}$$

As such equation (5) can be written as

$$\frac{c^{A}}{k}\frac{\partial\psi}{\partial t} = \nabla^2\psi \tag{18}$$

or

$$\frac{c_{vol}}{k}\frac{\partial\psi}{\partial t} = \nabla^2\psi + S \tag{19}$$

where S is given in equation (16).

Total enthalpy

From equation (7) we can write

$$\nabla T = \nabla H/c_{vol} - \delta H\,\nabla g_l/c_{vol}$$

Substitution in equation (5) will result in a governing equation in terms of total enthalpy, H,

$$\frac{\partial}{\partial t}(H) = \nabla\cdot(\Gamma\nabla H) + \nabla\cdot(\Gamma\,\delta H\,\nabla g_l) \tag{20}$$

where $\Gamma = k/c_{vol}$. Alternative examples of this form of governing equation can be found in the work of Cao *et al.*[31] and Mundim and Fortes.[32] The more common practice, however, in making a substitution of T in terms of H (or vice versa) is to make it after the discretization of the governing equation (5).[33–35] This approach will be discussed further in the numerical solution section.

A general governing equation

All the governing equations suitable for a fixed grid numerical solution presented so far can be written in the general form

$$c\frac{\partial\phi}{\partial t} = \nabla\cdot(\alpha\nabla\phi) + Q \tag{21}$$

where ϕ is the unknown variable, c is a specific heat, α is a diffusion coefficient and Q is a source term. The appropriate values of ϕ, c and Q for the given governing equations, equations (13), (15), (18), (19) and (20), are provided in Table I.

For the sake of consistency in the remainder of this text, it is convenient to express the basic governing equation (5) in the given general form. This can simply be achieved on associating the source term Q with the diffusive term $\nabla\cdot(k\nabla T)$ and setting $\alpha = 0$, see line 1 in Table I.

THE DISCRETIZATIONS

In discussing the possible numerical discretization approaches we concentrate attention on equation (21). For spatial discretization we concentrate attention on two-dimensional domains

Table I. Possible governing equations which can be used in a fixed grid solution

The general equation: $c\,\partial\phi/\partial t = \nabla\cdot(\alpha\nabla\phi) + Q$

1. *Basic equation* (equation (5))
   $\phi = H;\ c = 1;\ \alpha = 0;\ Q = \nabla\cdot(k\nabla T)$
2. *Apparent heat capacity* (equation (13))
   $\phi = T;\ c = c^{A} = c_{vol} + \delta H\ \mathrm{d}g_l/\mathrm{d}T;\ \alpha = k;\ Q = 0$
3. *Source* {equations (15) and (16)}
   $\phi = T;\ c = c_{vol};\ \alpha = k;\ Q = S = -\delta H\ \partial g_l/\partial t$
4. *Kirchhoff (No. 1)* (equation (18))
   $\phi = \psi;\ c = (c_{vol} + \delta H\ \mathrm{d}g_l/\mathrm{d}T)/k;\ \alpha = 1;\ Q = 0$
5. *Kirchhoff (No. 2)* (equation (19))
   $\phi = \psi;\ c = c_{vol}/k;\ \alpha = 1;\ Q = S = -\delta H\ \partial g_l/\partial t$
6. *Total enthalpy* (equation (20))
   $\phi = H;\ c = 1;\ \alpha = \Gamma = k/c_{vol};\ Q = \nabla\cdot(\Gamma\ \delta H\ \nabla g_l)$

Note: Mixture volumetric enthalpy $H = g_s H_s + g_l H_l$
Mixture conductivity $k = g_s k_s + g_l k_l$
Mixture volumetric specific heat $c_{vol} = g_s\rho_s c_s + g_l\rho_l c_l$

and employ either a Galerkin weighted residual finite element method[36] or a control volume based finite difference method.[30] The time discretization is based on the two level backward Euler (fully implicit) scheme. This choice of time integration scheme has been found to be efficient and stable[3] for a wide number of problems. In addition, its simplicity facilitates illustration of the various methods in the following discussions.

Finite elements

In the finite element method the domain of interest is discretized into a fixed mesh of elements. Typically, the elements are triangles, quadrilaterals or polyhedrons with node points at vertices for simple elements and additional node points at mid-planes when higher order approximations are used. Figure 3 shows a section of a typical finite element grid consisting of the elements associated with a node point P. The unknown variable is approximated over the entire domain R by

$$\phi(x, y, t) = \mathbf{N}(x, y)\cdot\boldsymbol{\phi}(t) \tag{22}$$

where $\mathbf{N}$ is the vector of interpolation (shape) functions N_P and $\boldsymbol{\phi}$ is the vector of nodal unknowns ϕ_P. The shape functions are chosen such that $N_P = 1$ at node P, $0 < N_P < 1$ in the area defined by the elements common to node P (i.e. the area of support) and $N_P = 0$ elsewhere. Using the

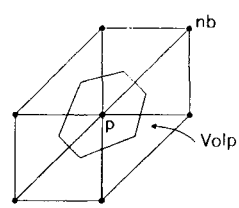

Figure 3. The region of support for node P in a mesh of triangular finite elements

Galerkin approach of weighted residuals, the spacewise discretization of equation (21) results in the matrix equations

$$\mathbf{C}(\phi)\frac{\mathrm{d}}{\mathrm{d}t}\boldsymbol{\phi} + \mathbf{K}(\phi)\boldsymbol{\phi} = \mathbf{F}(\boldsymbol{\phi}) \tag{23}$$

Using a backward Euler time discretization, the above equation becomes

$$(\mathbf{C} + \Delta t\mathbf{K})\boldsymbol{\phi} = \mathbf{C}\boldsymbol{\phi}^{\mathrm{old}} + \mathbf{F} \tag{24}$$

where Δt is the time step, the superscript $[\ ]^{\mathrm{old}}$ indicates evaluation at the old time level and all other evaluations are made at the current time level. Neglecting contributions from boundary conditions, the elements of $\mathbf{C}$ and $\mathbf{K}$ can be expressed as[36]

$$C_{ij} = \int_R c\,N_i N_j \mathrm{d}R \tag{25}$$

$$K_{ij} = \int_R \alpha \nabla N_i \nabla N_j \mathrm{d}R \tag{26}$$

A further refinement, which is often used in finite element modelling of phase change problems, is to use a so called 'lumped capacity' formulation. Essentially, in this approach the capacitance matrix $\mathbf{C}$ becomes a diagonal matrix. One lumping approach involves using the element node points as the only integration points, resulting in a capacitance matrix with elements

$$c_{ij} = \begin{cases} 0; & \text{if } i \neq j \\ c_i \displaystyle\int_R N_i; & \text{if } i = j \end{cases} \tag{27}$$

The effect of this lumped formulation is to associate with each node point a 'control volume', Vol_P, over which nodal values are representative, see Figure 3. Dalhuijsen and Segal[3] provide justification for the lumped formulation on noting that it is computationally advantageous and avoids oscillations in numerical solutions when used in conjunction with the backward Euler scheme.

For each specific version of the governing equation the matrices $\mathbf{C}$ and $\mathbf{K}$ can be generated on setting α and c to the values listed in Table I, followed by evaluation of the appropriate integrals given in equations (25)–(27). The vector $\mathbf{F}$, in equation (24), will depend on the nature of the source term Q. Specific versions of $\mathbf{F}$ are listed in Table II. Calculation of the global matrix elements C_{ij} and K_{ij} through the evaluation of the integrals in equations (25)–(26) is referred to as the assembly step. This can be achieved on a node by node basis, evaluating the integrals over the appropriate regions of support.[37] The more common practice, however, is to express the global integral equations, equations (25) and (26), as the sum of element integrals and assemble the equations on an element by element basis.[36]

Control volumes

Based on the structured grid illustrated in Figure 4, a fully implicit control volume integration[30] of the governing equation (21) results in the finite difference scheme

$$a_P\phi_P = a_W\phi_W + a_E\phi_E + a_N\phi_N + a_S\phi_S + b_P\phi_P^{\mathrm{old}} + \mathrm{Vol}_P Q_P \tag{28}$$

Table II. Versions of the source vector **F** in the finite element scheme equation (24)

1. *Basic equation*

   $\mathbf{F} = -\Delta t \mathbf{K}^* \mathbf{T}$

   where **T** are the nodal temperatures and the elements of $\mathbf{K}^*$ are

   $K^*_{ij} = \int_R k \nabla N_i \nabla N_j \, dR$

2. *Apparent heat capacity*

   $\mathbf{F} = 0$

3. *Source*

   $\mathbf{F} = \mathbf{M}(g_l^{old} - g_l)$

   where **M** is a diagonal matrix with elements

   $M_{PP} = \mathrm{Vol}_P \, \delta H_P$

   and $\mathrm{Vol}_P = \int_R N_P \, dR$

4. *Kirchhoff (No. 1)*

   $\mathbf{F} = 0$

5. *Kirchhoff (No. 2)*

   See Source method (line 3)

6. *Total enthalpy*

   $\mathbf{F} = -\Delta t \mathbf{K}^+ g_l$

   where g_l are the nodal liquid fractions and the elements of $\mathbf{K}^+$ are

   $K^+_{ij} = \int_R \{(k \, \delta H)/c_{vol}\} \nabla N_i \nabla N_j \, dR$

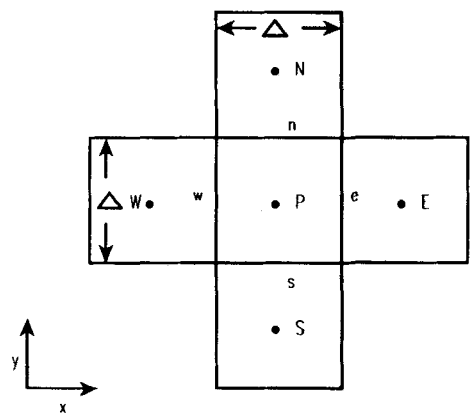

Figure 4. A structured arrangement of control volumes

where Vol_P is the volume of the control volume. The coefficients in equation (28) take the form

$$a_E = \Delta t \alpha_e, \quad a_W = \Delta t \alpha_w, \quad a_S = \Delta t \alpha_s \quad \text{and} \quad a_N = \Delta t \alpha_n \tag{29}$$

where the lower case subscript indicates evaluation on the faces of control volume surrounding node point P,

$$b_P = \mathrm{Vol}_P \, c_P \tag{30}$$

and

$$a_P = \sum_{nb} a_{nb} + b_P \tag{31}$$

where *nb* indicates the neighbouring nodes with influence on node P (E, W, S and N in the current case). The derivation of equation (28) implies a structure to the grid which is a common feature of a control volume formulation. This is not universal, however; for example, element by element techniques[38,39] may result in unstructured grids, with general form

$$a_P \phi_P = \sum_{nb} a_{nb} \phi_{nb} + b_P \phi_P^{\text{old}} + \text{Vol}_P Q_P \tag{32}$$

The neighbouring coefficient in equation (32) has the form

$$a_{nb} = \Delta t \, \eta \, \alpha \tag{33}$$

where η is a factor which is a function of the geometry of the control volumes. If nodes P and *nb* share a common control volume face, orthogonal to the line joining nodes P and *nb*, η can be defined as the ratio of the area of the common face to the distance between the nodes. The definition of the nodal source term, Q_P, in equation (32) depends on the form of the governing equation. Appropriate definitions of Q_P are given in Table III.

Table III. Definitions of the nodal source term Q_P

1. *Basic equation*	$Q_P = a_P^* T_P - \sum_{nb} a_{nb}^* T_{nb}$ where $a_{nb}^* = \Delta t \eta k$, $a_P^* = \sum_{nb} a_{nb}^*$
2. *Apparent heat capacity*	$Q_P = 0$
3. *Source*	$Q_P = \text{Vol}_P \, \delta H_P ([g_l]_P^{\text{old}} - [g_l]_P)$
4. *Kirchhoff (No. 1)*	$Q_P = 0$
5. *Kirchhoff (No. 2)*	See Source method (line 3)
6. Total enthalpy	$Q_P = a_P^+ [g_l]_P - \sum_{nb} a_{nb}^+ [g_l]_{nb}$ where $a_{nb}^+ = \Delta t \eta \{(k \, \delta H)/c_{\text{vol}}\}$, $a_P^+ = \sum_{nb} a_{nb}^*$

η is a geometric factor

Comments

The finite element scheme (equation (24)) has been written in a matrix form whereas the finite difference scheme (equation (32)) has been written in a point form. This choice is made with respect to convention. It is strongly stressed, however, that the finite element scheme can be written in a point form, and by a similar token, the finite difference scheme can be written in a matrix form. In fact, when linear right triangular elements and lumping are used, the resulting finite element discretized equation, equation (24), has the same form as the control volume discretized equation, equation (28). The equation systems become identical when the thermal properties are constant and the lumping used is such that Vol_p is a square.[38] The potential commonality between the finite element discretization and the control volume discretization will be emphasized extensively in the discussion of the various solution approaches.

SOLUTION PRELIMINARIES

A multitude of different schemes for fixed grid numerical solution of heat conduction controlled phase change problems can be found in the literature. The preceding sections of this paper have shown that the most common methods are based on a single governing equation, viz. equation (21). Furthermore, the discretization of this equation by either finite element or finite difference produces similar systems of non-linear equations (equation (24) or equation (32)). In the present study, we will not attempt to categorize all possible solution approaches based on equations (24) or (32) but rather concentrate on some basic and important techniques. To this end, attention is restricted to the following examples.

1. The basic formulation, equation (5)[33–35]
2. The apparent heat capacity formulation, equation (13)[20–26]
3. The source term formulation, equations (15) and (16)[6,9,27]

These formulations, the associated discretizations and the resulting solutions schemes can be considered to be representative of the range of possibilities.

Note that, in further discussions, a distinction will not be drawn between finite element and finite difference schemes. A distinction will be drawn, however, between solution schemes based on the matrix form of the discrete equations and those based on a point form of these equations.

Matrix form

In matrix form the discrete equations are:

1. The basic formulation

$$\mathbf{CH} + \Delta t\mathbf{K}^*\mathbf{T} = \mathbf{CH}^{\mathrm{old}} \tag{34}$$

2. The apparent capacity method

$$(\mathbf{C} + \Delta t\mathbf{K})\,\mathbf{T} = \mathbf{CT}^{\mathrm{old}} \tag{35}$$

3. The source method

$$(\mathbf{C} + \Delta t\mathbf{K})\,\mathbf{T} = \mathbf{CT}^{\mathrm{old}} + \mathbf{M}(\mathbf{g}^{\mathrm{old}} - \mathbf{g}) \tag{36}$$

In equations (34)–(36) the matrix $\mathbf{K}^*$ is defined in Table II, the matrices $\mathbf{K}$ and $\mathbf{C}$ are defined in equations (26) and (27) on choosing appropriate values for α and c from Table I and the diagonal matrix $\mathbf{M}$ is defined in Table II. Alternatively, the matrices in equations (34)–(36) can be obtained

using the coefficients, b_P, a_P and a_{nb} defined by equations (30), (31) and (33) respectively (see equations (40) and (41) below).

Point form

In point form the discrete equations are:

1. The basic formulation

$$H_P = H_P^{\text{old}} + (a_P^* T_P)/\text{Vol}_P + \left[\sum_{nb} (a_{nb}^* T_{nb})\right]/\text{Vol}_P \tag{37}$$

2. The apparent capacity method

$$a_P T_P = \sum_{nb} a_{nb} T_{nb} + b_P T_P^{\text{old}} \tag{38}$$

3. The source method

$$a_P T_P = \sum_{nb} a_{nb} T_{nb} + b_P T_P^{\text{old}} + \text{Vol}_P \, \delta H_P([g_l]P^{\text{old}} - [g_l]P) \tag{39}$$

In equations (37)–(39) the coefficients a_P^* and a_{nb}^* are defined in Table III and the coefficients b_P, a_P and a_{nb} can be defined by equations (30), (31) and (33) respectively. Alternatively, these coefficients can be associated with the matrix forms given by equations (34)–(36) such that

$$\begin{aligned} a_P^* &= \Delta t K_{PP}^* \\ a_{nb}^* &= \Delta t K_{Pj}^* \quad (j = 1, 2, \ldots, p-1, p+1, \ldots, n) \end{aligned} \tag{40}$$

$$\begin{aligned} b_P &= C_{PP} \\ a_P &= \Delta t K_{PP} + C_{PP} \\ a_{nb} &= \Delta t K_{Pj} \quad (j = 1, 2, \ldots, p-1, p+1, \ldots, n) \end{aligned} \tag{41}$$

SOLUTIONS: THE BASIC FORMULATION

Successive substitution

With reference to the point form of the basic scheme, equation (37), a common approach is a Gauss–Seidel point iteration with successive substitution. A recent description, based on a finite difference discretization, is provided by Shamsundar and Rooz.[35] In the case of a phase change occurring between temperatures T_l and T_s with no jump discontinuities equation (7) can be inverted and linearized to give

$$T = A(T)H + B(T) \tag{42}$$

where

$$A(T) = 1/\overline{c_{\text{vol}}}; \quad B(T) = -g_l \rho_l L/\overline{c_{\text{vol}}} \tag{43}$$

and

$$\overline{c_{\text{vol}}}\, T = g_s \int_{T_{\text{ref}}}^{T} \rho_s c_s \, \mathrm{d}\theta + g_l \int_{T_{\text{ref}}}^{T} \rho_l c_l \, \mathrm{d}\theta \tag{44}$$

Using equation (42) a point iterative scheme can be developed from equation (37), viz.

$$H_P = \frac{\mathrm{Vol}_P\, H_P^{\mathrm{old}} + a_P^*\, B(T_P) + \sum(a_{nb}^*\, T_{nb})}{\mathrm{Vol}_P + a_P^*\, A(T_P)} \tag{45}$$

In using this scheme, the nodal domain is 'swept' in a systematic manner and the most current iterative values are used.

If a step discontinuity occurs in the H vs. T (or g_l vs. T) curve at a given fixed temperature, modification of the iterative approach is required. The nodal enthalpy field is checked at each iteration. If the current value of H_P falls within the limits of H that define the jump then the nodal temperature T_P is set to the fixed temperature for the next iteration.[27,35]

The performance of equation (45) can be improved by using over-relaxation. Shamsundar and Rooz[35] note that for full efficiency this over-relaxation should be applied only at nodes away from the phase change. Using this approach they report a greater than two-fold improvement in convergence rates for two-dimensional problems.

Alternative, but similar point schemes, can be found in the work of Furzeland,[40] who employs an inner Newton iteration step to improve convergence, and Raw and Schneider,[33] who achieve 'spectacular convergence' for a restricted class of problems. The point schemes of this class have been reviewed by Voller.[27,41]

Newton linearization

In solving the matrix form of the basic scheme, equation (34), a possible approach is to use a Newton linearization.[34] In the case of a phase change occurring between temperatures T_l and T_s with no jump discontinuities, equation (42) can be substituted into equation (34) to give

$$[\mathbf{C} + \Delta t\mathbf{KA}]\mathbf{H} = \mathbf{C}\mathbf{H}^{\mathrm{old}} - \Delta t\mathbf{KB} \tag{46}$$

where $\mathbf{A}$ is a diagonal matrix with components $A(T_P)$ and $\mathbf{B}$ is a vector with components $B(T_P)$. We seek an iterative solution of the non-linear equation (46) in the form

$$\mathbf{H}^{k+1} = \mathbf{H}^k + \Delta\mathbf{H}^{k+1} \tag{47}$$

where the subscript k represents the iteration level. Using a Newton linearization, the following equation is derived for calculating the enthalpy update:

$$\mathbf{J}^k\, \Delta\mathbf{H}^{k+1} = -\mathbf{R}^k \tag{48}$$

where

$$\mathbf{R}^k = [\mathbf{C} + \Delta t\mathbf{KA}]\mathbf{H} - \mathbf{C}\mathbf{H}^{\mathrm{old}} + \Delta t\mathbf{KB} \tag{49}$$

and

$$\mathbf{J}^k = \partial\mathbf{R}^k/\partial\mathbf{H}^k = [\mathbf{C} + \Delta t\mathbf{KA}] \tag{50}$$

In practice, at the start of an iteration the residual $\mathbf{R}^k$ and the Jacobian $\mathbf{J}^k$ are calculated from equations (49) and (50). Then the linear equation (48) is solved for $\Delta\mathbf{H}^{k+1}$ and the enthalpy field updated via equation (47). Note that in the strict sense the proposed technique does not use a full Newton linearization since the calculation of the Jacobian $\mathbf{J}$ neglects variations of $\mathbf{A}$ and $\mathbf{B}$ with $\mathbf{H}$. Further, when a jump discontinuity is present in the H vs. T curve appropriate modifications have to be made in the calculation of the Jacobian $\mathbf{J}$ and the residual $\mathbf{R}$.

SOLUTIONS: APPARENT HEAT CAPACITY

The apparent capacity formulation, given in discrete form by equation (35) (matrix) or equation (38) (point), has many attributes. Of principal importance is the consistency of the equations with

basic finite element and control volume heat conduction solvers. The major problem in using such methods is in specifying an accurate numerical approximation for the rapidly changing apparent specific heat, c^A, equation (9). In order to illustrate how the numerical approximation of c^A is achieved, we choose the extreme case of an isothermal phase change at temperature T_m. However, the approximation methods introduced in this way are also applicable to the general phase change defined in Figure 2.

Consider an isothermal phase change occurring at temperature T_m. To avoid problems associated with the jump in the $g_l(T)$ at $T = T_m$, a small artificial temperature region is introduced and g_l is approximated by the linear piecewise continuous curve

$$g_l = \begin{cases} 1 & \text{if } T > T_m + \varepsilon \\ (T - T_m + \varepsilon)/(2\varepsilon) & \text{if } T_m - \varepsilon < T \leqslant T_m + \varepsilon \\ 0 & \text{if } T_m - \varepsilon \leqslant T \end{cases} \tag{51}$$

where ε is small temperature value. Owing to the rapid change in dg_l/dT, the apparent specific heat, c^A, calculated on substitution of equation (51) into equation (9) will contain a 'spike' about the phase change temperature, T_M. Unless some action is taken, this spike can lead to an erroneous solution in that latent heat effects are lost because the chosen time step allows the spike peak to skip a node point. The basic approach in overcoming this problem rests on selecting optimum values of ε, space step and time step. As a general rule, decreasing the time and space steps and increasing the value of ε will reduce the risk that the latent heat spike will jump a node. Bonacina and Comini[42] suggest as a 'rule of thumb', that two to three node points be maintained within the phase change range. Such a situation, however, may require a computationally demanding small time step or a large artificial temperature range that will not correctly reflect the physics of the problem. This situation can be alleviated on adopting a suitable numerical approximation for c^A. The aim of such an approximation is to allow efficient choices of time and space steps with small choices of the temperature range ε. Many numerical approximations for c^A have been suggested in the literature.[20–26] Recent reviews and investigations can be found in References 2, 3, 5, 7 and 8. In general, two classes of approximations can be identified:

1. Those based on space averaging, e.g. the method proposed by Lemmon[22]

$$c^A = \left[\frac{\nabla H \nabla H}{\nabla T \nabla T} \right]^{0.5} \tag{52}$$

   where the ∇H is numerically approximated in the same way as ∇T. With equation (52), it is possible that c^A will be discontinuous at a given node point. In a node by node assembly,[37] a weighted average value of c^A needs to be calculated. In an element by element assembly,[36] however, a nodal averaged value of c^A (weighted according the contribution made by the surrounding elements to the nodal volume Vol_P) will occur naturally.
2. Those based on temporal averaging, e.g. Morgan *et al.*[23]

$$c^A = \frac{H - H^{\text{old}}}{T - T^{\text{old}}} \tag{53}$$

In the case of a backward Euler time integration, the discrete equation (equation (35) or (38)) is non-linear and hence an iterative solution strategy needs to be adopted. In practice, this strategy can be based on successive substitution or Newton linearization. With an explicit time integration scheme, the discrete equations are linear and can be solved in one step.

In general, use of a numerical approximation for c^A will lead to efficient and accurate solutions with small values of ε. Modifications that improve the performance include the following.

1. A post iterative correction to adjust the nodal temperatures to balance the latent heat evolved in the previous iteration.[25,26] This step ensures a full accounting of the latent heat evolution. The result is that efficient and accurate results can be obtained with a very small temperature interval, ε.
2. As written, equation (51) will result in a 'top hat' function for c^A which involves sharp and rapid changes at either end of the temperature range. The rapid change in c^A can be reduced on redefinition of equation (51) such that the resulting 'top hat' function has sloping as opposed to vertical sides. The sharp changes in c^A can be reduced on redefinition of equation (51), such that the liquid fraction temperature curve is C_1 continuous as opposed to C_0 continuous.[43]

Some further remarks are made concerning apparent heat capacity formulations.

1. Although the apparent heat capacity methods have been presented in the context of an isothermal problem it is noted that these methods work best in the case of a naturally occurring wide phase change interval.
2. Apparent heat capacity methods have been primarily used in conjunction with finite element techniques. This does not preclude them from finite difference solutions.[24]
3. In equation (35), recall that C is a diagonal matrix with elements given by $c_P^A \, \mathrm{Vol}_P$. In the case of an isothermal phase change, at nodes where the phase change exists, c^A will take a large value. This will 'force' changes in the nodal temperature to be small, as required (i.e. $T_P \approx T_P^{\mathrm{old}} = T_m$). As a result, in isothermal problems the iterative solution of the matrix equations is 'inherently stable'.

SOLUTIONS: SOURCE METHODS

A basic method

Source based methods, based on equations (36) and (39), have gained popularity over the years.[6,9,27] This is due to the fact that a wide range of phase change phenomena (e.g. convection[9] and solute transport) can be easily handled. In using a source based method, one needs to note that the inverse of the liquid fraction–temperature relationship, $T = F^{-1}(g_l)$ (see equation (8) and Figure 2), will always be a well posed function. In particular, at an isothermal phase change the temperature $T = T_m$ whenever the local liquid fraction, g_l, lies *strictly* in the interval [0, 1]. Using this observation the following iterative solution of equation (36) can be applied.

1. At time level n, assume that the temperature, T, and liquid fraction fields, g_l, are known and that the values at time level $n + 1$ need to be determined.
2. The source term, $\mathbf{M}(\mathbf{g}^{\mathrm{old}} - \mathbf{g})$, is approximated using the best estimate for the nodal liquid fractions, $[g_l]_P$.
3. With step 2 equation (36) will be linear in the latent heat terms and can be solved in any chosen manner (e.g. a direct solver).
4. On solution of the linearized equations the predicted temperature field will not necessarily be consistent with the current liquid fraction field. For example, in an isothermal phase change the predicted nodal temperatures $T_P \neq T_m$ when $[g_l]_P$ lies in the interval [0, 1]. In such a case, the value of the nodal liquid fraction is updated so that on subsequent iterations (repetitions of steps 2 and 3) the predicted nodal temperature is 'driven' to T_m.

The 'key' to the source based iteration is the method by which the liquid fraction field, g_l, is updated. A number of updating schemes suitable for a wide range of problems are suggested in

the literature.[6,9,27,44] On considering the point form given in equation (39), a simple and robust scheme suitable for the general phase change system of Figure 2 can be derived. After the kth application of a matrix solver, the point form of the source formulation can be arranged as

$$a_P T_P = \sum_{nb} (a_{nb} T_{nb}) + b_P T_P^{\text{old}} + \text{Vol}_P \delta H_P ([g_l]_P^{\text{old}} - [g_l]_P) \tag{54}$$

where the most current iterative values are used. If the phase change is occurring about the Pth node (i.e. $0 < [g_l]_P < 1$) then the kth estimate of nodal temperature should be such that $T_P = F^{-1}([g_l]_P)$. To achieve this the kth estimate of the liquid fraction, $[g_l]_P$, needs to be corrected such that

$$a_P F^{-1}([g_l]_P) = \sum_{nb} (a_{nb} T_{nb}) + b_P T_P^{\text{old}} + \text{Vol}_P \delta H_P ([g_l]_P^{\text{old}} - [g_l]_P - [\Delta g_l]_P) \tag{55}$$

where $[\Delta g_l]_P$ is the required correction. Subtracting equation (55) from equation (54) the correction can be approximated as

$$[\Delta g_l]_P = a_P \frac{T_P - F^{-1}([g_l]_P)}{\text{Vol}_P \delta H_P} \tag{56}$$

thus leading to the liquid fraction update

$$[g_l]^{k+1} = [g_l]^k + \lambda [\Delta g_l]_P \tag{57}$$

where the parameter λ is an under-relaxation factor which is required if convergence is to be achieved.[9] In the strict sense, this liquid fraction update should be applied only at nodes where the phase change is occurring. In practice, however, the liquid fraction update is applied during each iteration and *at every node*. After the application of the liquid fraction update, to account for the fact that equation (57) is not appropriate at every node an 'over/under-shoot' correction

$$g_l = \begin{matrix} 0 & \text{if } [g_l]^{k+1} < 0 \\ 1 & \text{if } [g_l]^{k+1} > 1 \end{matrix} \tag{58}$$

is used. This step will ensure that a full accounting of the latent heat evolution is made. Unlike apparent heat capacity methods, this full accounting is achieved with no additional accuracy restrictions on the size of the time step. In general, when accounting for the latent heat evolution, the time steps used in source methods can be larger than those used in apparent heat capacity methods.

In the source scheme presented above, the iterative solution of the system of linear equations does not contain the same stabilizing mechanism found in the solution of the apparent heat capacity equations. Essentially, the diagonal of the coefficient matrix does not naturally contain large forcing values. As a result, unless under-relaxation is wisely applied the iterative procedure may not converge. Practical experience with both control volume discretizations with line by line solvers[9,27] and finite elements with direct solvers[44] indicates that a relaxation value in the range $\lambda = 0{\cdot}5$–$0{\cdot}7$ will provide efficient convergence for both one- and two-dimensional problems.

A linearized source method

Recently Voller[27] has proposed a source based scheme for isothermal problems that does result in large diagonal terms in the coefficient matrix. The basic feature of this approach can be viewed as a source linearization. For illustrative purposes consider the point form of the discrete equation given in equation (32). An efficient solution is often obtained if the source term Q_P is

linearized[30] as

$$Q_P = S_p T_P + S_c \tag{59}$$

where the S_p term is taken to the left hand side of the equation and absorbed in the a_P coefficient (i.e. the diagonal of $\mathbf{C}$). Up to this point, in the source terms introduced in this paper $S_p = 0$. This does not have to be the case, however. On reference to the apparent heat capacity method, the source term S in equation (16) can be written as

$$S = -\delta H \frac{dg_l}{dT} \frac{\partial T}{\partial t} \tag{60}$$

Taking guidance from Morgan *et al.*[23] the term dg_l/dT is approximated as

$$\beta(g_l - g_l^{old})$$

where $\beta = 1/(T - T^{old})$. In implementation, when g_l lies strictly in the range [0, 1] β is given an arbitrary large negative value (-10^9 say). With this approach, at nodes where the phase change is occurring, the source term, Q_P, in equation (32) can be linearized according to equation (59) such that at a given node P,

$$\begin{aligned} S_p &= \beta_P \delta H_P [g_l]_P^{old} \\ S_c &= -S_p T_m + \delta H_P [g_l]_P^{old} - \delta H_P [g_l]_P \end{aligned} \tag{61}$$

On using this linearized source term, the discrete equations will almost be identical to that given in equation (54). The important difference is that the diagonal elements of the coefficient matrix corresponding to nodes which are changing phase will contain a large value. This value will 'stabilize' the solution by forcing the linear equations to yield the correct nodal temperatures. In practice, the steps in one iteration are as follows.

1. At the start of the iteration the local liquid fraction field, g, is checked. At nodes where the phase change is occurring the equations are modified according to (61).
2. Solution of the modified equations is then carried out.
3. After solution of the equations the liquid fraction field is updated. The update formula can be derived in the same manner used in the basic source scheme, equations (56) and (57), resulting in

$$[g_l]^{k+1} = [g_l]^k + a_P \frac{T_P - T_m}{\mathrm{Vol}_P \delta H_P} \tag{62}$$

Application of equation (62) is made at every node followed by the over/under shoot correction (equation (58)). On comparing equations (57) and (62), it is important to note that the a_P coefficient in equation (62) can be much larger and that the under-relaxation has been dropped.

This improved source technique for isothermal phase change problems has been implemented in both finite difference[27] and finite element solutions.[44] In a range of one-dimensional test problems Voller[27] was able to report rapid convergence (one or two iterations). Work is on going to extend this approach to non-isothermal phase change systems.[44]

The linearized source scheme can be regarded as a 'generic' scheme, in that appropriate choice of S_p and S_c results in a variety of solution approaches. Furthermore, the scheme can be used as a natural 'bridge' between source based methods and apparent heat capacity methods. Consider the following alternatives for equation (61). If

$$\begin{aligned} S_p &= 0 \\ S_c &= \delta H_P ([g_l]_P^{old} - [g_l]_P) \end{aligned} \tag{63}$$

the basic source scheme results. On the other hand, if

$$S_p = \beta_P \delta H_P([g_l]_P^{old} - [g_l]_P)$$
$$S_c = -S_p T_P^{old} \tag{64}$$

the apparent heat capacity scheme with the Morgan *et al.*[23] approximation for c^A results.

ADDITIONAL COMMENTS

The purpose of this section is to make some general comments related to modelling and analysis of phase change problems.

Time stepping

In the discretizations presented in the current work, the time stepping has been restricted to the backward Euler (fully implicit) two level scheme. Choice of a time stepping method, however, can play a significant role in the ultimate accuracy and efficiency of the method. Other two level schemes that can be used[2,3,45] include the Crank–Nicolson and forward Euler (fully explicit). Three level schemes have also been employed.[2,3,25,45] The forward Euler and three level schemes are noteworthy since they do not require iteration within a time step. Use of such schemes, however, leads to a restriction in the choice of the time step. Thus, these methods are more suited to apparent capacity methods which require small time steps due to accuracy considerations. Time stepping methods that require iterations within each time step are best suited for source based methods.

Two important approaches, which can also be classified as time stepping methods are:

1. The implicit/explicit algorithm:[4,46,47] in essence, in parts of the domain where slow changes occur, an explicit time integration is used whereas in the thermally active regions, stability is maintained on using an implicit time integration.[4,46,47] The advantage of this approach is that the size and bandwidth of the system of equations are reduced without any significant loss of accuracy. This approach has been effectively used in simulation of sand mould castings.[46]
2. 'Alternating-direction' finite element methods:[4,48] this approach is based on factorizing the shape functions into directional parts. As a consequence, the matrix equations are factorized into directional components with very narrow bandwidths which lead to efficient solutions.[4,48]

Adaptive methods

In the case of a distinct solid/liquid phase change, an alternative to a fixed grid solution approach is to use a front tracking method. The aim of such an approach is to ensure that a line of node points will always coincide with the solid/liquid interface. This is desirable in that high gradients and discontinuities at this interface can be readily resolved. Front tracking can be achieved on using a transformed grid[49] or deforming elements.[35] Although front tracking is outside the scope of the present study, a number of hybrid fixed grid and deforming grid methods have been proposed which are worth noting. Crivelli and Idelsohn[50,51] use a fixed grid formulation, i.e. equation (21). Improvements in the accuracy are achieved, however, on local splitting of the finite elements which are changing phase into solid and liquid components. A similar philosophy is adopted by Tacke[52] in one-dimensional finite difference solutions. Lewis

et al.[53] and Lacroix and Voller[49] have proposed an adaptive grid technique in which a fine discretization is always present in the vicinity of the phase change. This adaptive grid is based on the fixed grid governing equations which removes the constraint that a grid line must lie on the phase front. In this way an area of fine grid can be moved such that it approximately follows the phase change.

Handling of irregular geometries

An important difference between finite element and finite difference methods, which far overshadows their differences in deriving the nodal equations, is the nature by which these equations are assembled. Control volume methods[30] often exploit extremely rapid 'line by line' solution algorithms, which take advantage of the structured nature of the grid in constructing the system of equations. Building this structure into the solution method, however, imposes restrictions on the geometries that can be modelled or requires the application of boundary fitted co-ordinates.[54] On the other hand a finite element method assembles the nodal equations on an element by element basis. This will mean that fast structured solution methods cannot be applied but that arbitrary geometries can be more easily dealt with. This comment also applies to unstructured forms of the finite difference method.[38,39]

Temperature dependent conductivity

Many practical problems involve thermal properties that will vary with temperature. In terms of representing the conductivity this can lead to difficulties. The Kirchhoff formulations given in Table I offer a means by which such problems can be solved by apparent heat capacity or source techniques. Alternatively, the given schemes in terms of temperature T can be used and a careful means of evaluating the thermal conductivities in a numerical element can be devised.[4,54] Recently Tamma and Namburu[55] have proposed a formulation in which the diffusion term in the governing equation is written in terms of the heat flux $q = k\nabla T$. This provides a natural means for variations in thermal conductivity to be absorbed into the finite element equations and also allows a direct introduction of non-linear boundary conditions.

CONCLUSIONS

In the numerical modelling of solidification phase change systems one of the central issues is the latent heat evolution. Many successful approaches are available. This paper has attempted to identify and categorize the major and most widely used methods. The choice of any one method over the others will depend on the problem at hand and the experience and preference of the user. As such, it is not possible to identify a single best method or group of methods. However, it is worthwhile to list some attributes of a 'good' method for the analysis and simulation of phase change problems. These include:

1. Applicability to three dimensions and arbitrary geometries.
2. Ability to deal with the general liquid fraction temperature curve given in Figure 2.
3. Ease of implementation into existing computer codes (including grid generation and post processing software)
4. Ability to deal with non-constant thermal properties and all types of boundary conditions.
5. Ability to couple additional effects and phenomena like convection, electromagnetic forces, solute transport, microstructural evolution.
6. Reasonable computational efficiency and accuracy.

In general, both the apparent heat capacity and source based methods have the potential to incorporate the above attributes. This is reflected in current research in the modelling phase change process and phenomena in which the apparent heat capacity[2,4,7,45,46] and source based methods[6,8–12] are by far the most widely used.

The development of numerical techniques to deal with phase change systems is a viable area for research. In terms of numerical analysis, many questions related to accuracy and efficiency have not yet been resolved. In addition, the development of efficient solvers for the non-linear equations resulting from phase change problems is currently an area of considerable interest. In an engineering context the central challenge is to expand the basic conduction techniques so that more of the phenomena associated with phase changes can be incorporated into numerical models. This research requires the development of both sophisticated numerical approaches and suitable models of the underlying physics.

ACKNOWLEDGEMENTS

V. R. Voller would like to acknowledge the Minnesota Super Computer Institute for a resources grant. B. G. Thomas would like to acknowledge the National Science Foundation for supporting this research: NSF–MSS–8957195.

APPENDIX

Nomenclature

a	coefficients in nodal equations (equations (31), (33), (41))
a^*	coefficients (Table III, equation (40))
b	coefficients in nodal equations (equations (30), (41))
A, B	temperature linearization constants (equations (42), (43))
c	generalized heat capacity (Table I)
$\mathbf{C}$	finite element capacitance matrix with terms C_{ij} (equation (25) or (27))
c_{vol}	volume-averaged specific heat of mixture (equation (10))
$\overline{c_{\text{vol}}}$	linearized c_{vol} (equation (44))
c^{A}	apparent specific heat coefficient, (J/kg K) (equation (9))
Δg	phase fraction correction (equation (55))
$\mathbf{F}$	finite element force vector with terms F_i (Table II)
F	liquid fraction–temperature function (Figure 2, equation (8))
g	phase fraction (solid or liquid)
H	total volumetric enthalpy (J/m^3) (equations (3), (7), Table I)
H^*	volumetric enthalpy inside REV (J/m^3) (equation (2))
δH	difference between solid and liquid enthalpy (equation (11))
ΔH	enthalpy correction (J/m^3) (equation (48))
$\mathbf{J}$	Jacobian matrix (equation (50))
k	thermal conductivity of mixture (equation (6))
$\mathbf{K}$	finite element conductivity matrix with terms K_{ij} (equation (26))
$\mathbf{K}^*$	modified $\mathbf{K}$ (Table II)
L	volumetric latent heat of solidification (J/m^3)
$\mathbf{M}$	source matrix containing terms M_{ii} (Table II)
$\mathbf{N}$	vector containing finite element shape functions, N_i (equation (22))
Q	generalized heat source (Tables I, III)

R domain of interest
$\mathbf{R}$ residual vector (equation (49))
REV representative elementary volume (m^3)
S volumetric heat source (W/m^3) (equation (16))
S_c constant portion of linearized source term (equation (61))
S_p gradient of linearized source term (equation (61))
T temperature (°C)
T_m unique melting temperature (°C)
T_{ref} reference temperature (°C)
t time (s)
Δt time step size (s)
$\mathbf{u}$ vector containing material velocities (m/s)
V volume (equations (1), (2))
Vol_P volume of control volume associated with node P
$\mathbf{X}$ vector defining position of centroid of REV (equation (2))
$\mathbf{x}$ vector defining position within REV (equation (2))
x, y co-ordinate directions (m)
α generalized thermal diffusion coefficient (Table I)
β $1/(T - T_{old})$ (equation (60))
Γ k/c_{vol}
ε small temperature difference (equation (51))
η geometric factor relating nodes P and nb
θ integration parameter (equations (7), (11), (17))
λ under-relaxation factor
ρ density (kg/m^3)
ϕ unknown variable (Table I)
ψ Kirchhoff temperature (equation (17))

Subscripts (pertaining to material type or location)

s pertaining to solid
l pertaining to liquid
nb pertaining to neighbouring nodes of influence of node P
P pertaining to typical node point, P
N, S, E, W north, south, east, west node points
[ ] used to separate multiple subscripts

Superscripts (pertaining to time integraton)

k iteration number (within time step)
old previous time level

REFERENCES

1. J. Crank, *Free and Moving Boundary Problems*, Clarendon Press, Oxford, 1984.
2. B. G. Thomas, I. V. Samarasekara and J. K. Brimacombe, 'Comparison of numerical modeling techniques for complex two-dimensional, transient heat conduction problems', *Metall. Trans. B*, **15**, 307–318 (1984).
3. A. J. Dalhuijsen and A. Segal, 'Comparison of finite element techniques for solidification problems', *Int. j. numer. methods eng.*, **23**, 1807–1829 (1986).
4. R. W. Lewis and P. M. Roberts, 'Finite element simulation of solidification problems', *Appl. Sci. Res.*, **44**, 61–92 (1987).
5. D. Porier and M. Salcudean, 'On numerical methods used in the mathematical modeling of phase change in the liquid metals', ASME paper 86-WA/HT-22 (1986).

6. M. Salcudean and Z. Abdullah, 'On the numerical modeling of heat transfer during solidification processes', *Int. j. numer. methods eng.*, **28,** 445–473 (1988).
7. J. A. Dantzig, 'Modelling liquid–solid phase changes with melt convection', *Int. j. numer. methods eng.*, **28,** 1769–1785 (1989).
8. M. Rappaz, 'Modelling of microstructure formation in solidification processes', *Int. Mater. Rev.*, **34,** 93–123 (1989).
9. A. D. Brent, V. R. Voller and K. J. Reid, 'Enthalpy porosity technique for modelling convection–diffusion phase change: Application to the melting of a pure metal', *Numer. Heat Transfer*, **13,** 297–318 (1988).
10. W. D. Bennon and F. P. Incropera, 'The evolution of macro-segregation in statically cast binary ingots', *Metall. Trans. B*, **18,** 611–612 (1987).
11. C. Beckermann and R. Viskanta, 'Double-diffusive convection during dendritic solidification of a binary mixture', *PCH*, **10,** 195–213 (1988).
12. V. R. Voller, A. D. Brent and C. Prakash, 'The modelling of heat, mass and solute transport in solidification systems', *Int. J. Heat Mass Transfer*, **32,** 1719–1731 (1989).
13. J. A. Dantzig, 'Thermal stress development in metal casting processes', *Met. Sci. Tech.*, 7(3) (1989) (in press).
14. D. M. Stefanescu and C. S. Kanetkar, 'Modeling microstructural evolution of eutectic cast iron and of the gray/white transition', *Trans. AFS*, **95,** 139–144 (1987).
15. F. J. Bradley, Cai Jum and M. H. Zmerli, 'Numerical simulation of the solidification of eutectic ductile iron casting alloys', in R. W. Lewis and K. Morgan (eds.), *Proc. Conf. on Numerical Methods in Thermal Problems*, 1989, pp. 267–279.
16. C. Beckermann, 'Melting and solidification of binary mixtures with double-diffusive convection in the melt', *Ph.D. Dissertation*, Purdue Univ., Indiana, 1987.
17. Y. Bachmat and J. Bear, 'Macroscopic modelling of transport phenomena in porous media: 1. The continuum approach', *Transport Porous Media*, **1,** 213–240 (1986).
18. J. Bear and Y. Bachmat, 'Macroscopic modelling of transport phenomena in porous media: 2. Applications to mass, momentum and energy transport', *Transport Porous Media*, **1,** 213–240 (1986).
19. T. W. Clyne, 'Numerical modeling of directional solidification of metallic alloys', *Met. Sci.*, **16,** 441–450 (1982).
20. G. Comini, S. Del Giudice, R. W. Lewis and O. C. Zienkiewicz, 'Finite element solution of nonlinear heat conduction problems with spectral reference to phase change', *Int. j. numer. methods eng.*, **8,** 613–624 (1974).
21. S. Del Giudice, G. Comini and R. W. Lewis, 'Finite element simulation of freezing processes in soils', *Int. j. numer. anal. methods geomech.*, **2,** 223–235 (1978).
22. E. C. Lemmon, 'Phase change techniques for finite element codes', in R. W. Lewis and K. Morgan (eds). *Proc. Conf. on Numerical Methods in Thermal Problems*, 1979, pp. 149–158.
23. K. Morgan, R. W. Lewis and O. C. Zienkiewicz, 'An improved algorithm for heat conduction problems with phase change', *Int. j. numer. methods eng.*, **12,** 1191–1195 (1978).
24. J. S. Hsiao, 'An efficient algorithm for finite-difference analysis of heat transfer with melting and solidification', *Numer. Heat Transfer*, **8,** 653–666 (1985).
25. Q. T. Pham, 'The use of lumped capacitance in the finite element solution of heat conduction problems with phase change', *Int. J. Heat Mass Transfer*, **29,** 285–291 (1986).
26. G. Comini, S. Del Giudice and O. Saro, 'Conservative equivalent heat capacity methods for nonlinear heat conduction', in R. W. Lewis and K. Morgan (eds.), *Proc. Conf. on Numerical Methods in Thermal Problems*, 1989, pp. 5–15.
27. V. R. Voller, 'A fast implicit finite difference method for the analysis of phase change problems', *Numer. Heat Transfer*, (in press).
28. W. D. Rolph III and K. J. Bathe, 'An efficient algorithm for analysis of nonlinear heat transfer with phase changes', *Int. j. numer. methods eng.*, **18,** 119–134 (1982).
29. J. Roose and O. Storrer, 'Modelization of phase changes by fictitious heat flow', *Int. j. numer. methods eng.*, **20,** 217–225 (1984).
30. S. V. Patankar, *Numerical Heat Transfer and Fluid Flow*, McGraw-Hill, New York, 1980.
31. Y. Cao, A. Fagiri and W. S. Chang, 'A numerical analysis of Stefan problem for generalized multi-dimensional phase change structures using the enthalpy model', *Int. J. Heat Mass Transfer*, **22,** 1289–1298 (1989).
32. M. J. Mundim and M. Fortes, 'Accurate finite element method of solution of phase change problem based on enthalpy diffusion', in R. W. Lewis and K. Morgan (eds.), *Proc. Conf. on Numerical Methods in Thermal Problems*, 1989, pp. 90–100.
33. M. J. Raw and G. E. Schneider, 'A new implicit solution procedure for multidimensional finite-difference modeling of the Stefan problem', *Numer. Heat Transfer*, **8,** 559–571 (1985).
34. R. E. White, 'A nonlinear parallel algorithm with application to the Stefan problem', *SIAM J. Numer. Anal.*, **23,** 639–653 (1986).
35. N. Shamsundar and E. Rooz, 'Numerical methods for moving boundary problem', in W. J. Minkowycz *et al.* (eds.), *Handbook of Numerical Heat Transfer*, Wiley, New York, 1988.
36. O. C. Zienkiewicz, *The Finite Element Method*, McGraw-Hill, New York, 1977.
37. T. M. Shih, *Numerical Heat Transfer*, Hemisphere, Washington, 1984.
38. I. Ohnaka and T. Fukusako, 'Calculation of the solidification of castings by a matrix method', *Trans. Iron Steel Inst. Japan*, **17,** 410–418 (1977).
39. B. R. Baliga and S. V. Patankar, 'Elliptic Systems: Finite element method II', in W. J. Minkowycz *et al.* (eds.),

Handbook of Numerical Heat Transfer, Wiley, New York, 1988.
40. R. M. Furzeland, 'A comparative study of numerical methods for moving boundary problems', *J. Inst. Math. Applic.*, **26**, 411–429 (1980).
41. V. R. Voller, 'Implicit finite-difference solutions of the enthalpy formulation of the Stefan problem', *IMA J. Numer. Anal.*, **5**, 201–214 (1985).
42. C. Bonacina and G. Comini, 'On the solution of the nonlinear heat conduction equation by the numerical methods', *Int. J. Heat Mass Transfer*, **16**, 581–589 (1973).
43. J. Szekely and R. G. Lee, 'The effect of slag thickness on heat loss from ladles holding molten steel', *Trans. Met. Soc. AIME*, **242**, 961–965 (1968).
44. C. R. Swaminathan, 'On fixed grid approaches for modeling solidification problems', *MS Report, University of Minnesota*, 1990.
45. M. Hogge, 'A comparison of two and three level integration schemes for nonlinear heat conduction', in R. W. Lewis *et al.* (eds.), *Numerical Methods in Heat Transfer*, Wiley, Chichester, U.K., 1981.
46. M. Sammonds, K. Morgan and R. W. Lewis, 'Finite element modelling of solidification in sand castings employing an implicit–explicit algorithm', *App. Math. Mod.*, **9**, 170–174 (1985).
47. M. R. Tadayon, R. W. Lewis and K. Morgan, 'An implicit–explicit finite element microcomputer program for transient heat conduction analysis', in B. A. Schrefler and R. W. Lewis (eds.), *Microcomputers in Engineering Applications*, Wiley, New York, 1987.
48. R. W. Lewis, K. Morgan and P. M. Roberts, 'Application of an alternating-direction finite element method to heat transfer problems involving a change of phase', *Numer. Heat Transfer*, **7**, 471–482 (1984).
49. M. Lacroix and V. R. Voller, 'Finite difference solutions of solidification phase change problems: Transformed versus fixed grids', *Numer. Heat Transfer*, in press.
50. L. A. Crivelli and S. R. Idelsohn, 'A temperature based finite element solution for phase change problems', *Int. j. numer. methods eng.*, **23**, 99–119 (1986).
51. L. A. Crivelli and S. R. Idelsohn, 'Making curved interfaces straight in phase change problems', *Int. j. numer. methods eng.*, **24**, 375–393 (1987).
52. K. H. Tacke, 'Discretization of the explicit enthalpy method for planar phase change', *Int. j. numer. methods eng.*, **21**, 543–554 (1985).
53. R. W. Lewis, H. C. Huang and A. S. Usmani, 'Remeshing approaches to finite element simulation of casting problems', presented in *Heat Transfer in Phase Change Problems, Eurotherm Seminar 6*, 1988.
54. W. C. Schreiber, 'The numerical simulation of heat conduction in irregularly-shaped materials of thermally dependent properties', *Int. j. numer. methods eng.*, **30**, 679–696 (1990).
55. K. K. Tamma and R. R. Namburu, 'Recent advances and trends in enthalpy based Lax–Wendroff/Taylor–Galerkin finite element formulation for application to solidification problems', in R. W. Lewis and K. Morgan (eds.), *Proc. Conf. on Numerical Methods in Thermal Problems*, 1989, pp. 267–279.